*International Journal of Computational and Experimental Science and ENgineering (IJCESEN)*

*Vol. 11-No.3 (2025) pp. 4491-4499*
*http://www.ijcesen.com*

**ISSN: 2149-9144**



**Research Article**

# Accurate Detection of Basal Cell Carcinoma Using Fuzzy U-Net and Deep Learning on Dermoscopic Images

**Dhiyanesh B[1], Kiruthiga G[2], Shakkeera L[3]*, Syed Umar[4], Anusuya V[5]**

[1]SRM Institute of Science and Technology, Associate Professor, CSE, Vadapalani campus, Chennai, Tamil Nadu India
**Email:** dhiyanu87@gmail.com - **ORCID:** 0000-0002-6786-8096

[2]Karpagam College of Engineering, Professor, IT, Coimbatore, Tamil Nadu India.
**Email:** kiruthiga.g@kce.ac.in - **ORCID:** 0000-0003-1969-9838

[3]Presidency University, Professor/CSE, Bengaluru, Karnataka, India.
* **Corresponding Author Email:** shakkeera.l@presidencyuniversity.in - **ORCID:** 0000-0002-7216-3269

[4]Marwadi University, Professor/CSE, Rajkot, Gujarat, India.
**Email:** umar332@gmail.com - **ORCID:** 0000-0002-9031-1560

[5]Ramco Institute of Technology, Associate Professor/IT, Rajapalayam, Tamil Nadu, India
**Email:** pgkrishanu@gmail.com - **ORCID:** 0000-0002-1366-0214

**Article Info:**

**DOI:** 10.22399/ijcesen.2475
**Received :** 28 February 2025
**Accepted :** 17 May 2025

**Keywords**

BCC
wiener filter
fuzzy U-Net segmentation
DNN

**Abstract:**

Basal cell carcinoma (BCC) is a common kind of skin cancer that is distinguished by the presence of telangiectasias, which are tiny blood veins that resemble trees and are frequently seen inside skin lesions. Precise recognition of these characteristics is essential for prompt diagnosis and successful therapy. Deep learning (DL) models have advanced in skin cancer imaging in recent years, increasing the accuracy of diagnosis and feature segmentation. The ISIC 2019 dataset, a comprehensive collection of dermoscopic pictures covering a variety of skin lesions, including BCC, was employed in our suggested approach. Our approach started with applying a Wiener filter to denoise the images. This preprocessing step significantly improved image quality, making critical features more discernible and facilitating subsequent analysis. After denoising, we implemented the Fuzzy U-Net model for image segmentation. This model excels at accurately delineating lesions, providing precise boundaries that are essential for effective classification. A deep neural network (DNN) was then trained using the segmented pictures, enabling it to differentiate basal cell carcinoma from other skin diseases by identifying important characteristics. We used common assessment measures including precision of 97%, F1 score of 98%, and AUC of 0.99% and testing accuracy of 97.47% to assess our model's performance. The outcomes show that our method is reliable and successful, with a high level of accuracy in detecting basal cell cancer. In addition to expediting the diagnostic procedure, this approach may enhance patient outcomes by enabling earlier discovery and treatment.

## 1. Introduction

In the United States, around two million instances of BCC are found annually. As part of the first BCC diagnosis, a dermatologist or mid-level physician (physician assistant or nurse practitioner) would visually evaluate the patient, often using a dermatoscope. Invasive treatment, such as a biopsy, is undertaken if the diagnosis is not obvious or confirmation is required [1]. Given the greater depth of invasion of the disease, locally damaging nature, and therapeutic challenges for more severe cases, early identification of BCC is crucial. Furthermore, BCCs could be more likely to metastasize; if treatment is delayed, the likelihood might rise to 1% to 2% for cancers bigger than 3 cm in diameter and as much as 50% for those less than 10 cm. A skin lesion is an abnormal development or appearance of the skin that surrounds the surrounding skin. There are two types of skin lesions: primary and secondary. A primary skin lesion is an abnormal skin condition that may be present from birth or develop over time. The development or alteration of initial skin lesions may give rise to subsequent skin lesions. Scratching a mole until it bleeds causes a scab to form, which results in a secondary skin lesion [2].

To find abnormalities in the skin, doctors employ a variety of imaging methods, including spectroscopy [3], optical coherence tomography, thermography, multispectral imaging, wide-field imaging [4], and ultrasound. Nonetheless, digital dermoscopy a digital color snapshot enlarged by a dermoscope is the most widely used and straightforward kind of imaging. Dermatologists use a variety of dermoscopic criteria or high-level characteristics, together with dermoscopic images, to diagnose basal cell carcinoma. The most accurate clinical criteria are for basal cell carcinoma. The following are dermoscopic criteria for basal cell carcinoma regions: colds inside colds (concentration system), absent brown reticular lines (pigment network), bluish-gray nodules of different sizes (egg nests, spheres, and convex points), branching and linear vessels (arborescent and superficial telangiectasias), and leaf-shaped radial lines connected to a common base.

Dermatologists advise one of three treatments, depending on the type of skin lesion: medication, surgery, or at-home care. Even if they appear harmless, certain skin lesions can cause a lot of anxiety in patients since they might be cancerous and require surgery to eradicate. Melanoma, the most fatal type of skin cancer, may be curable in its early stages but becomes fatal after it has spread. Therefore, a comprehensive diagnosis of skin patches is required to protect patients' growth and provide timely treatment [5]. Automating the analysis through machine learning techniques could lead to a medical system and framework that assists with contextual relevance, enhances clinical reliability, helps doctors communicate objectively, reduces human fatigue errors, lowers mortality rates, lowers medical expenses, and makes disease identification easier. One step toward accomplishing these objectives is developing a machine-learning technique to distinguish between benign and malignant pigmented skin lesions [6].

The field of dermatological diagnostics has undergone a total transformation because to developments in medical imaging and computer methods, especially deep learning (DL). Deep neural networks (DNNs) provide a potent way to automate dermoscopic image processing, enabling quick and precise categorization of a range of skin lesions, including BCC. Researchers may train models to identify complex patterns and characteristics that would be invisible to the human eye by utilizing huge datasets, like the ISIC 2019 dataset. In this work, we provide a DNN-based system created especially for BCC classification from dermoscopic pictures. In our method, the pictures are preprocessed to improve quality, and then the lesions are effectively segmented. In order to accurately distinguish BCC from other skin disorders, the segmented pictures are then passed into a DNN for classification. In addition to increasing diagnostic precision, this approach seeks to offer a scalable solution that can support dermatologists in clinical settings.

Our work aims to show the effectiveness of DNNs in the automated identification of BCC through thorough assessment utilizing accepted performance criteria, eventually adding to the expanding corpus of research in computer-aided dermatology.

### 1.1 Organization of the work

The work of earlier writers on different forms of skin cancer and how machine learning and deep learning algorithms may be used to identify them is covered in Section 2. Our suggested method for basal cell carcinoma (BCC) is described in Section 3, along with the preprocessing, segmentation, and classification procedures used. The examination of BCC dermoscopic pictures is shown in Section 4, emphasizing the outcomes that our model generated. The main conclusions of our suggested BCC detection approach are finally outlined in Section 5, which also highlights the method's importance and possible influence on clinical practice.

## 2. Related work

Conventional techniques like dermoscopy and naked eye inspection have reduced the specificity of noninvasive diagnosis. An artificial intelligence model based on deep learning was created to identify BCC in reflectance confocal microscopy pictures automatically. The model's repeatability and generalizability were demonstrated by its respective areas under 89.7% and 88.3% [7]. Additionally, the study extracts input patterns from skin images using statistical features and Gray Level Co-occurrence Matrix approaches. K-nearest neighbor, Decision Tree, and Support Vector Machine classifiers are then used to categorize the models; SVM outperforms the other classifiers by an approximate margin [8]. It shows the effectiveness of an attention-based artificial neural network (ANN) in detecting basal cell carcinomas (BCCs) in histological whole-slide images. When compared to pathologists' eye-tracking data, the ANN correctly diagnosed tumor areas, with a ROC curve area under the curve of 0.993 [9]. An automated technique for identifying basal cell carcinoma in EVCM photographs based on deep learning algorithms may help with the diagnosis. A model trained on the EVCM dataset had a diagnostic accuracy rate of 92%, which is comparable to the H&E model. This method might help diagnose basal cell carcinoma during Mohs surgery [10]. To train an ANN using reflectance confocal microscopy (RCM) imaging to improve the specificity of Raman spectroscopy (RS) in the identification of BCC. To select hair and epidermis structure images with high accuracy, the network inputs two ResNet50 networks with 191 RCM images [11].

The ML algorithm's overall classification accuracy for labeled data was 99.0%, while for unlabelled tissue sections, it was 99.9%. 189 signals were assigned tentative metabolite identifications, indicating the possibility of diagnosis [12]. When given extra color and texture information, the classifier outperforms a CNN that uses the original image input. The outcomes of the earlier texture measurements are enhanced by a new color co-occurrence matrix. This method has a sensitivity of 0.99, a specificity of 0.94, and an accuracy of 0.97 when determining whether a lesion is basal cell carcinoma or not [13]. Hematoxylin and eosin-stained pathology slides' 258 digital histology pictures were used to develop the Mask-RCNN (Mask Region-based CNN) model. The model was identified as basal cell carcinoma after 1000 epochs of training [14]. Because it causes local damage, basal cell carcinoma, a common non-melanoma skin cancer, should be detected early and treated promptly. CNN and a SVM activation layer were used in a study that combined multispectral imaging and artificial intelligence to detect basal cell carcinoma and healthy cell signals with up to 90% accuracy [15]. The method uses high-frequency ultrasound, optical coherence tomography, and diffuse reflectance spectroscopy [16].

Skin cancers are common all over the world, and the kind and stage of the malignancy upon diagnosis affect the prognosis and disease burden. It was demonstrated that melanoma, squamous cell carcinoma, and basal cell carcinoma had acceptable diagnostic accuracy. 14,224 AI/ML systems were evaluated for the early detection of skin cancer [17]. In an attempt to increase diagnosis accuracy, researchers looked at a variety of machine learning models, such as convolutional neural networks (CNNs), Gaussian functions, and conventional data models. According to the findings, CNN-based algorithms performed better than conventional models, which makes them an excellent option for dermatologists and oncologists looking for an early diagnosis [18].

***Table 1.*** *Comparison of Existing literatures*

| S.No | Author and year | Methods | Results |
|---|---|---|---|
| 1. | Akanksha Maurya et al., (2024) [1] | Topological Data Analysis (TDA)-Deep Learning (DL), EfficientNet-B5 | 97.4% accuracy, AUC is 0.995 |
| 2. | Veronika et al., (2022) [20] | Basal cell carcinoma (BCC), MobileNet | Specificity 85%, sensitivity 46% |
| 3. | Jairo Hurtado and Francisco Reales., (2021) [21] | ABCD dermatological criteria, ANN (Artificial neural network) | Accuracy 87.1% |
| 4. | Xuemei Lan et al., (2024) [22] | multi-head self-attention (MSA) U-Net | Precision is 0.910, recall is 0.869, dice score is 0.889, and IoU is 0.800 |
| 5. | Stephen et al., (2021) [23] | Natural Language Processing (NLP), GATE (generic architecture for text engineering) | mean accuracy, recall, and F1 score of 86.0%, 84.2%, and 84.5%, |
| 6. | Bhuvaneshwari et al., (2022) [24] | HAM10000 dataset, Convolutional Neural Network (CNN) | 95.18% accuracy |
| 7. | FilmonYacob et al., (2023) [25] | CNN | Accuracy 93.5% |
| 8. | Lixin Liu et al., (2022) [26] | Random forest (RF) | accuracy = 0.952 ± 0.014, kappa value= 0.928 ± 0.022 |
| 9. | Beshatu et al., (2022) [27] | EffecientNetB0, MobileNetv2, ResNet50, VGG16 | Accuracy of EffecientNetB0, MobileNetv2, ResNet50, VGG16 95.3%, 97.1%, 89.8%, and 89.9% |
| 10. | Mustafa., (2022) [28] | KNN (k nearest neighbor) | 98% of accuracy |
| 11. | Roshni Thanka et al., (2023) [29] | VGG16 and XGBoost | Maximum 99.1% accuracy |
| 12. | Ngan Thanh Luu et al., (2021) [30] | RF (random forest) | Accuracy 93% |

This study uses color and texture to identify skin problems using the Hue-Saturation-Value (HSV) properties of entropy, variance, and maximum histogram value. Decision Tree with Support Vector Machine learning techniques are used to classify skin illnesses, and the proposed system's performance accuracy is evaluated [19].

## 3. Proposed methodology

The proposed method for classifying basal cell carcinoma (BCC) uses a robust pipeline combining the Wiener filter, fuzzy U-net segmentation, and deep neural network (DNN) classification. Initially, a Wiener filter is used to downsample BCC images, improving their quality by reducing noise while preserving essential features. Following this, the Fuzzy U-Net model is used for effective image segmentation, which enables accurate delineation of lesions from the background. This section is important for accurately identifying and analyzing the features of BCC. Finally, a DNN is used for classification and trained on segmented images to distinguish BCC from other skin conditions. The results of this comprehensive technique are evaluated using metrics such as precision, recall, F1 score, and precision, which show how well it performs in diagnosing BCC based on significant clinical criteria. Figure 1 depicts the general architecture of the suggested BCC.

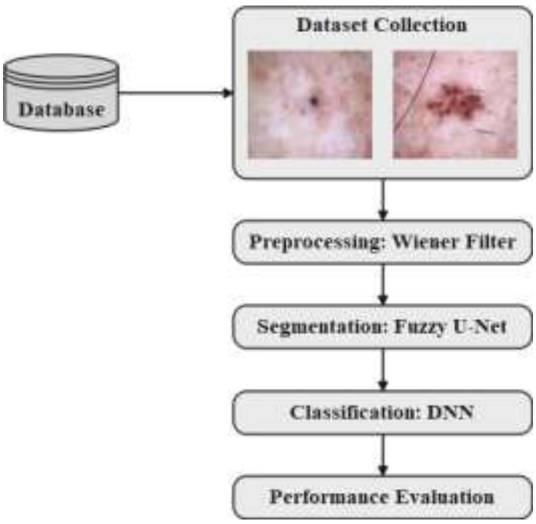


***Figure 1.*** *Flow diagram of Proposed BCC classification*

### 3.1 Dataset

This collection consists of 2357 photos of benign and malignant oncological illnesses and was produced by the International Skin Imaging Collaboration (ISIC) 2019. All photos were arranged using the classification derived from the ISIC, with the exception of melanomas and moles, which are very common. Each subgroup was then split up into an equal number of photos.

### 3.2 Preprocessing: Wiener filter

Applying the Wiener filter eliminates noise in the dermoscopic BCC images. The Wiener filter is a strong technique for image denoising that works especially well at improving the quality of noise-affected photos while maintaining crucial features. BCC pictures frequently contain different kinds of noise, particularly when they are taken dermoscopically. Images become crisper when this noise is reduced with the Wiener filter. The most likely technique for picture denoising is displayed below.

$$\hat{I} = \hat{I}\,(x,y) - \frac{\sigma_y^2}{\widehat{\sigma_y^2}}(\hat{I}(x,y) - \widehat{\mu_L}) \qquad (1)$$

Here,
$\hat{I}\,(x,y) - corrupted\ image$
$\sigma_y^2 - noise\ variance$
$\widehat{\mu_L} -$
$local\ mean\ on\ the\ pixel\ window\ of\ the\ image$
$\widehat{\sigma_y^2} - local\ variance$
In the instance when the noise variance throughout the picture equals 0, then $\sigma_y^2$= 0 = >$\hat{I}\,(x,y)$. The local variance is greater than the global variance and the ratio almost equals 1 when the global noise variance is less.
High local variance indicates the presence of edges in the picture frame under examination, while $\hat{I} = \hat{I}\,(x,y)$ if $\sigma_y^2 >> \widehat{\sigma_y^2}$ .The following is how the formulation works in this situation if the local and global variances match: As$\widehat{\sigma_y^2} \approx \sigma_y^2\ then\ \hat{I} = \widehat{\mu_L}$
Segmentation: fuzzy U-NET
Fuzzy U-net receives the pre-processed photos and superimposes them on the skin area. Upsampling and downsampling are the two components of the proposed system. Figure 2 shows the building of a fuzzy U-net.
The encoder and decoder networks are joined to form the U-net. In the conventional CNN that is used as the encoder, semantics are more significant than geography. Segmentation requires both spatial and semantic information. The U-net network's decoder collects semantic data from the network's lowest layer in order to extract particular information. The high-resolution features of the encoder element are immediately received by the decoder component, which then combines them to create accurate segment structures. Two convolutional layers make up the segmentation network utilized in this investigationThe convolutional operations are reversed in the

decoder, and these two layers are inserted within the pooling layers in the encoder. Batch normalizing is replaced with instance normalization, and the repaired linear unit (ReLU) modifies the rectified linear unit (ReLU). The top layer's batch size is 42 feature maps, and the patch size is 32x32 pixels. The goal of the four pooling processes is to efficiently train the whole slice. Assume that the input is yp on the lth layer and that the center pixel of each patch on the nth feature is (l, m).

$$q_{lmn}^{p}(t) = (W_h^g)^T\, y_p^{g(l,m)}(t) + (W_n^r)^T y_p^{r(l,m)}(t-1) + b_n \qquad (2)$$

$y_p^{g(l,m)}$ $and$ $y_p^{r(l,m)}$ $-$
$inputs\ of\ convolution\ neural\ layer$
$(W_h^g)^T$ $and$ $(W_n^r)^T$ $-$
$weights\ of\ the\ convolution\ layer$
$b_n - bias$

$$g(y1k1) = g\left[q_{lmn}^{p}(t)\right] = max[0, q_{lmn}^{p}(t)] \qquad (3)$$

In convolutional encoding and decoding, g(y1k1) represents the down and upsampling layers. Output from the CNN unit. This output is used for down- and up-sampling during encoding and decoding processes.

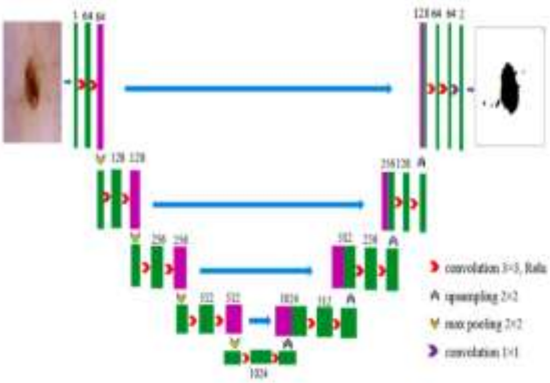


***Figure 2.*** *Fuzzy U-Net architecture*

**3.3 Classification: DNN (Deep neural network)**

Skin cancer is effectively identified by the DNN model using feature vectors in the final step of BCC classification. One of the traditional models of artificial neural networks (ANNs) is the DNN, which is a feed-forward neural network (FFNN). The DNN model's architecture is shown in Figure 2. The input, output, and hidden layers are its three layers. Networks receive pre-processed input datasets from the input layer. The number of input neurons is equal to the input characteristic that will be discussed later.

$$X = x_1, x_2, \dots, x_n \qquad (4)$$

Because DNN permits the insertion of one or more hidden layers, the hidden layer shows up later. The following formula is used to create the hidden layer map for the input X.

$$h_j = \sum_i w_i x_i + b_j \qquad (5)$$

$j - no. of\ hidden\ units,\ j = 1,2,3, \dots, k$
$b_j - bias$
$w_i - random\ weight$

Each hidden layer has a nonlinear activation function associated with it. In DNN models, ReLU expedites the training process and enhances results. The significant improvement of ReLU is demonstrated by the decrease in gradient vanishing and bursting problems. Despite non-differentiability and nonlinearity at zero, the rectifier neuron outperforms hyperbolic and sigmoid tangent neurons. Using a sparse representation with genuine zeros improves performance for sparse data sets. Tanh activation and sigmoid functions in binary classification performed better than ReLU for 50 epochs. ReLU performs better than sigmoid and tanh activation functions after 100 epochs. As a result, the authors choose to implement the described approach using the ReLU activation function. Equation (6) is used to formulate the hidden layer results.

$$h = f(h_j) \qquad (6)$$

here,

$$f(h_j) = ReLU(h_j) \qquad (7)$$

The output of DNN is calculated as,

$$\sigma(X)_j = \frac{e^{X_j}}{\sum_{k=}^{k} e^{X_k}} \qquad (8)$$

The j index (j = 1, 2, …, k) denotes the number of output units, whereas X represents the input vector to the output layer. The DNN model may train the network by mapping the input to the output of the corresponding class.

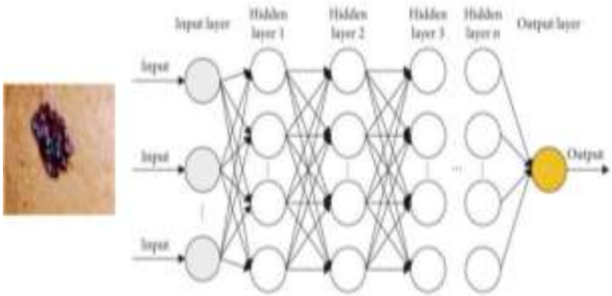


***Figure 3.*** *Architecture of DNN*

## 4. Result and discussion

The proposed BCC classification using DNN approach based on dermoscopic images. The wiener filter is used to enhance the picture's quality and look during the preprocessing phase in order to make illness detection easier through image processing. The Python programming language is used to implement it, and metrics such as mean square error (MSE), structural similarity index measurement (SSIM), and peak signal to noise ratio (PSNR) are assessed. Table 2.2 below shows the performance metrics for the various image sets of the ISIC dataset.

***Table 2.*** *Performance metrics*

| Dataset Details | Performance Metrics | | |
|---|---|---|---|
| | PSNR | MSE | SSIM |
| Training data set | 29.19 | 79.14 | 0.96 |
| Training ground truth dataset | 29.35 | 76.43 | 0.9421 |
| Testing dataset | 26.34 | 106.21 | 0.5431 |
| Testing ground truth dataset | 29.04 | 78.26 | 0.9901 |

Originally created for biomedical image segmentation, the U-Net architecture has become widely used in many different disciplines because of its strong capacity to segment pictures with high accuracy. Tasks requiring accurate object or region of interest segmentation and border identification are especially well-suited for U-Net. The figure 4 shows the input image of UNet architecture with skin cancer (BCC) and without skin cancer (non-BCC).

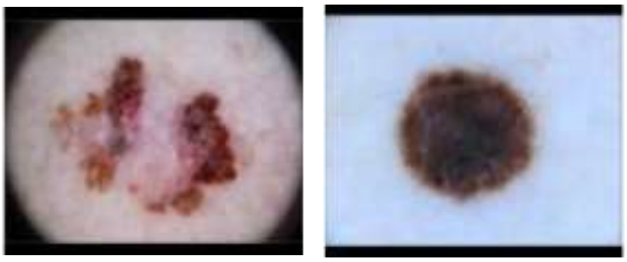

(a) BCC (b) Non-BCC

***Figure 4.*** *Input Image a) BCC, b) Non-BCC*

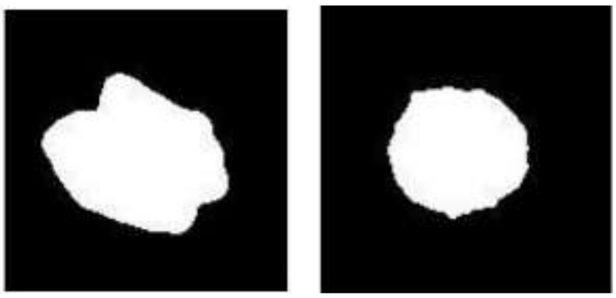

(a) (b)

***Figure 5.*** *Segmented image using U-Net a) BCC, b) Non-BCC*

The figure 5 shows the region of interested segmented and border identification image of BCC and Non-BCC using fuzzy U-Net architecture


***Figure 6.*** *ISIC dataset class image*

The dataset of ISIC consists three class. Each class consists training set, training ground truth set, testing set and testing ground truth set. The figure 6 shows the three class of basal cell carcinoma, melanoma and nevus.

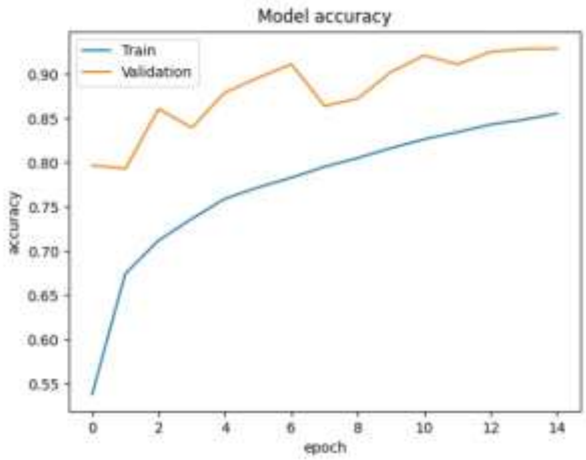


***Figure 7.*** *Proposed model accuracy vs epoch steps*

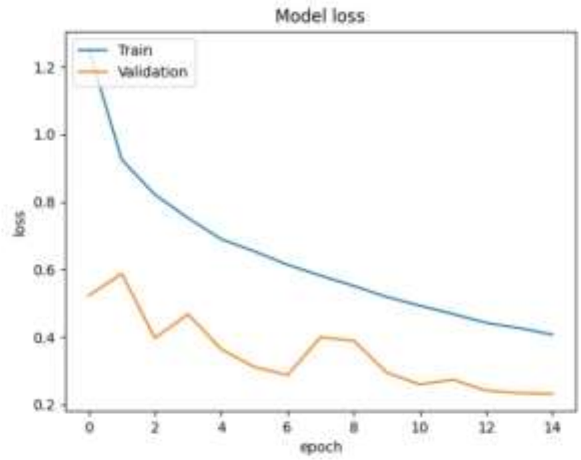


***Figure 8.*** *Proposed Deep Neural Network model loses vs epoch steps*

The deep neural network's model accuracy and model loss shown in figure 7 and figure 8.the graph shows the model accuracy for 15 epochs steps. The total test accuracy of proposed model is 97.91 % for 15 epoch steps. The figure 8 shows the Train and validation loss of proposed model. The losses are gradually decrease depends upon the epoch steps.

```
Performance Metrics
Test Accuracy                 : 97.47%
Precision                     : 97%
Sensitivity (BCC)             : 100%
Sensitivity (Melanoma)        : 96%
Sensitivity (Nevus)           : 98%
F1-score                      : 98%
AUC                           : 0.99
```

***Figure 9.*** *performance value of proposed DNN model.*

The performance metrics of proposed model get from the python implementation the figure. 9 shows the performance of DNN with individual class of ISIC dataset. the precision, sensitivity of each class, f1 score and AUC values are 97%, (100%, 96%,98%), 98% and 0.99

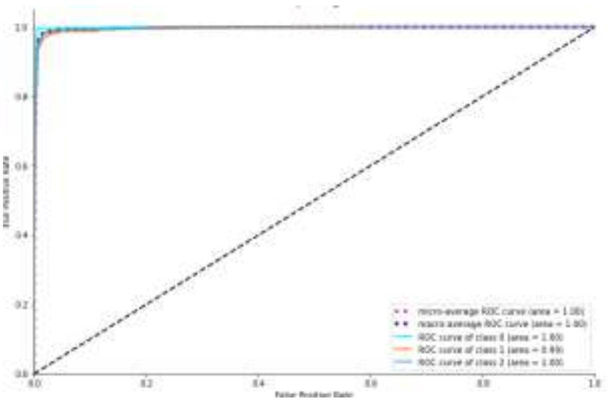

***Figure 10.*** *ROC curve of proposed DNN model*

The figure 10 shows the ROC curve of the proposed Deep Neural Network model. The ROC curve of BCC, Melanoma and Nevus are 1.00, 0.99 and 1.00. the value achieved by plot the graph between false positive rate and true positive rate.

## 5. Conclusion

In conclusion, the proposed approach to classify basal cell carcinoma (BCC) by integrating the Wiener filter, fuzzy U-net segmentation, and deep neural network (DNN) classification significantly improves automated skin cancer detection. We effectively reduced noise by applying a Wiener filter to improve image quality and clarified important features such as telangiectasia. The subsequent Fuzzy U-Net segmentation allowed lesions to be precisely drawn, ensuring that essential characteristics were accurately captured for analysis. Finally, the DNN classifier provided a strong distinction between BCC and other skin conditions, as verified by metrics such as precision of 97%, F1 score of 98%, and AUC of 0.99% and testing accuracy of 97.47%. This comprehensive methodology improves diagnostic accuracy and supports clinicians in making more informed decisions in patient care by underscoring the transformative potential of deep learning technologies in dermatology. Our approach paves the way for improved outcomes in the diagnosis and treatment of skin cancer.

## Author Statements:

- **Ethical approval:** The conducted research is not related to either human or animal use.
- **Conflict of interest:** The authors declare that they have no known competing financial interests or personal relationships that could have appeared to influence the work reported in this paper
- **Acknowledgement:** The authors declare that they have nobody or no-company to acknowledge.
- **Author contributions:** The authors declare that they have equal right on this paper.
- **Funding information:** The authors declare that there is no funding to be acknowledged.
- **Data availability statement:** The data that support the findings of this study are available on request from the corresponding author. The data are not publicly available due to privacy or ethical restrictions.

## References


[1] Maurya, A., Stanley, R. J., Lama, N., Nambisan, A. K., Patel, G., Saeed, D., et al. (2024). Hybrid Topological Data Analysis and Deep Learning for Basal Cell Carcinoma Diagnosis. *Journal of Imaging Informatics in Medicine.* 37; 92-106. https://doi.org/10.1007/s10278-023-00924-8

[2] Dhivyaa, C. R., Sangeetha, K., Balamurugan, M., Amaran, S., Vetriselvi, T., & Johnpaul, P. (2020). Skin lesion classification using decision trees and random forest algorithms. *Journal of Ambient Intelligence and Humanized Computing.* https://doi.org/10.1007/s12652-020-02675-8

[3] Fried, L., Tan, A., Bajaj, S., Liebman, T. N., Polsky, D., & Stein, J. A. (2020). Technological advances for the detection of melanoma. Advances in diagnostic techniques. *Journal of the American Academy of Dermatology.* 83; 983-992. https://doi.org/10.1016/j.jaad.2020.03.122

[4] Birkenfeld, J. S., Tucker-Schwartz, J. M., Soenksen, L. R., Aviles-Izquierdo, J. A., & Marti-Fuster, B. (2020). Computer-aided classification of suspicious pigmented lesions using wide-field images.

*Computer Methods and Programs in Biomedicine.* 195. https://doi.org/10.1016/j.cmpb.2020.105631

[5] Abbas, S., Jalil, Z., Javed, A. R., Batool, I., Khan, M. Z., Noorwali, A., et al. (2021). BCD-WERT: A novel approach for breast cancer detection using whale optimization based efficient features and extremely randomized tree algorithm. *PeerJ Computer Science.* 7. https://doi.org/10.7717/peerj-cs.390

[6] Gadamsetty, S., Ch, R., Ch, A., Iwendi, C., & Gadekallu, T. R. (2022). Hash-based deep learning approach for remote sensing satellite imagery detection. *Water.* 14. https://doi.org/10.3390/w14050707

[7] Campanella, G., Navarrete-Dechent, C., Liopyris, K., Monnier, J., Aleissa, S., Minhas, B., et al. (2022). Deep Learning for Basal Cell Carcinoma Detection for Reflectance Confocal Microscopy. *Journal of Investigative Dermatology.* 142; 97-103. https://doi.org/10.1016/j.jid.2021.06.015

[8] Ahammed, M., Mamun, M. A., & Uddin, M. S. (2022). A machine learning approach for skin disease detection and classification using image segmentation. *Healthcare Analytics.* 2. https://doi.org/10.1016/j.health.2022.100122

[9] Kimeswenger, S., Tschandl, P., Noack, P., Hofmarcher, M., Rumetshofer, E., Kindermann, H., et al. (2021). Artificial neural networks and pathologists recognize basal cell carcinomas based on different histological patterns. *Modern Pathology.* 34; 895-903. https://doi.org/10.1038/s41379-020-00712-7

[10] Sendin-Martin, M., Lara-Caro, M., Harris, U., Moronta, M., Rossi, A., Lee, E., et al. (2022). Classification of Basal Cell Carcinoma in Ex Vivo Confocal Microscopy Images from Freshly Excised Tissues Using a Deep Learning Algorithm. *Journal of Investigative Dermatology.* 142; 1291-1299. https://doi.org/10.1016/j.jid.2021.09.029

[11] Chen, M., Feng, X., Fox, M. C., Reichenberg, J. S., Lopes, F. C. P. S., Sebastian, K. R., et al. (2022). Deep learning on reflectance confocal microscopy improves Raman spectral diagnosis of basal cell carcinoma. *Journal of Biomedical Optics.* 27(6). https://doi.org/10.1117/1.jbo.27.6.065004

[12] Brorsen, L. F., McKenzie, J. S., Pinto, F. E., Glud, M., Hansen, H. S., Haedersdal, M., et al. (2024). Metabolomic profiling and accurate diagnosis of basal cell carcinoma by MALDI imaging and machine learning. *Experimental Dermatology.* 33. https://doi.org/10.1111/exd.15141

[13] Serrano, C., Laz, M., Serrano, A., Toledo-Pastrana, T., Barros-Tornay, R., & Acha, B. (2022). Clinically Inspired Skin Lesion Classification through the Detection of Dermoscopic Criteria for Basal Cell Carcinoma. *Journal of Imaging.* 8. https://doi.org/10.3390/jimaging8070197

[14] Dragomir, A. C., Cocuz, I. G., Cotoi, O. S., & Azamfirei, L. (2022). Artificial intelligence-based model for establishing the histopathological diagnostic of the cutaneous basal cell carcinoma. *Acta Marisiensis-Seria Medica.* 68(4). https://doi.org/10.2478/amma-2022-0020

[15] Courtenay, L. A., González-Aguilera, D., Lagüela, S., Del Pozo, S., Ruiz, C., Barbero-García, I., et al. (2022). Deep Convolutional Neural Support Vector Machines for the Classification of Basal Cell Carcinoma Hyperspectral Signatures. *Journal of Clinical Medicine.* 11(9). https://doi.org/10.3390/jcm11092315

[16] Surkov, Y. I., Serebryakova, I. A., Kuzinova, Y. K., Konopatskova, O. M., Safronov, D. V., Kapralov, S. V., et al. (2024). Multimodal Method for Differentiating Various Clinical Forms of Basal Cell Carcinoma and Benign Neoplasms In Vivo. *Diagnostics.* 14. https://doi.org/10.3390/diagnostics14020202

[17] Jones, O. T., Matin, R. N., van der Schaar, M., Bhayankaram, K. P., Ranmuthu, C. K. I., Islam, M. S., et al. (2022). Artificial intelligence and machine learning algorithms for early detection of skin cancer in community and primary care settings: a systematic review. The Lancet Digital Health, 4(6), e466–e476. https://doi.org/10.1016/s2589-7500(22)00023-1

[18] Alkhushayni, S., Al-zaleq, D., Andradi, L., & Flynn, P. (2022). The Application of Differing Machine Learning Algorithms and Their Related Performance in Detecting Skin Cancers and Melanomas. *Journal of Skin Cancer.* 2022. https://doi.org/10.1155/2022/2839162

[19] Raut, R., Borole, Y., Patil, S., Khan, V., & Takale, D. G. (2022). Skin Disease Classification Using Machine Learning Algorithms. *NeuroQuantology.* 20(10); 9624-9629. https://doi.org/10.48047/nq.2019.17.03.2011

[20] Shavlokhova, V., Vollmer, M., Gholam, P., Saravi, B., Vollmer, A., Hoffmann, J., et al. (2022). Deep Learning on Basal Cell Carcinoma In Vivo Reflectance Confocal Microscopy Data. *Journal of Personalized Medicine.* 12(9). https://doi.org/10.3390/jpm12091471

[21] Hurtado, J., & Reales, F. (2021). A machine learning approach for the recognition of melanoma skin cancer on macroscopic images. *TELKOMNIKA Telecommunication, Computing, Electronics and Control.* 19(4); 1357-1368. https://doi.org/10.12928/telkomnika.v19i4.20292

[22] Lan, X., Guo, G., Wang, X., Yan, Q., Xue, R., Li, Y., et al. (2024). Differentiation and risk stratification of basal cell carcinoma with deep learning on histopathologic images and measuring nuclei and tumor microenvironment features. *Skin Research and Technology.* 30. https://doi.org/10.1111/srt.13571

[23] Ali, S. R., Strafford, H., Dobbs, T. D., Fonferko-Shadrach, B., Lacey, A. S., Pickrell, W. O., et al. (2022). Development and validation of an automated basal cell carcinoma histopathology information extraction system using natural language processing. *Frontiers in Surgery.* 9. https://doi.org/10.3389/fsurg.2022.870494

[24] Shetty, B., Fernandes, R., Rodrigues, A. P., Chengoden, R., Bhattacharya, S., & Lakshmanna, K. (2022). Skin lesion classification of dermoscopic images using machine learning and convolutional

neural network. *Scientific Reports.* 12. https://doi.org/10.1038/s41598-022-22644-9

[25] Yacob, F., Siarov, J., Villiamsson, K., Suvilehto, J. T., Sjöblom, L., Kjellberg, M., et al. (2023). Weakly supervised detection and classification of basal cell carcinoma using graph transformer on whole slide images. *Scientific Reports.* 13. https://doi.org/10.1038/s41598-023-33863-z

[26] Liu, L., Qi, M., Li, Y., Liu, Y., Liu, X., Zhang, Z., et al. (2022). Staging of Skin Cancer Based on Hyperspectral Microscopic Imaging and Machine Learning. *Biosensors.* 12(10). https://doi.org/10.3390/bios12100790

[27] Wako, B. D., Dese, K., Ulfata, R. E., Nigatu, T. A., Turunbedu, S. K., & Kwa, T. (2022). Squamous Cell Carcinoma of Skin Cancer Margin Classification From Digital Histopathology Images Using Deep Learning. *Cancer Control.* 29; 1-16.

[28] Hatem, M. Q. (2022). Skin lesion classification system using a K-nearest neighbor algorithm. *Visual Computing for Industry, Biomedicine, and Art.* 5(7). https://doi.org/10.1186/s42492-022-00103-6

[29] Thanka, M. R., Edwin, E. B., Ebenezer, V., Sagayam, K. M., Reddy, B. J., Günerhan, H., et al. (2023). A hybrid approach for melanoma classification using ensemble machine learning techniques with deep transfer learning. *Computer Methods and Programs in Biomedicine Update.* 3. https://doi.org/10.1016/j.cmpbup.2023.100103

[30] Luu, N. T., Le, T. H., Phan, Q. H., & Pham, T. T. H. (2021). Characterization of Mueller matrix elements for classifying human skin cancer utilizing random forest algorithm. *Journal of Biomedical Optics.* 26(7). https://doi.org/10.1117/1.jbo.26.7.075001